

## Automatic Fault Diagnosis Technology of Roller Bearings of High-speed Rail Based on IFD and AE

Na Meng<sup>1</sup>, Sha Li<sup>1</sup>, Meizhu Li<sup>1</sup>, Jiang Wei<sup>1</sup> and Sheng Wang<sup>1,\*</sup>

<sup>1</sup>The Open University of Shaanxi, College of Mechanical and Electrical Engineering and Automotive Technology, Xi'an 710065, Shaanxi, China

### Abstract

**INTRODUCTION:** With the development of technology and policy support, high-speed rail's temporal and spatial layout is gradually expanding, and it becomes essential to ensure high-safety operation.

**OBJECTIVES:** The real-time correlation fault diagnosis technology of critical components of electromechanical systems of high-speed trains is analyzed, and a new method of automatic fault diagnosis based on genetic support vector machine is proposed.

**METHODS:** In this study, the Author combines two techniques, IFD and AE, and introduces an adaptive weighting algorithm to fuse the data of the two and experimentally verify their accuracy.

**RESULTS:** The experimental results show that in the IFD experiment, the 2-point frequency at 1050 speed is 347.6 Hz, and the 3-point frequency is 498.4 Hz, both of which are very close to the 2 and 3 times frequencies of the 1-point frequency, and the multiplicative relationship is much more straightforward.

**CONCLUSION:** Combining IFD and AE can realize automatic and accurate diagnosis of bearing state and pre-diagnosis of bearings by adaptive weighted fusion algorithm, which is effective in the practical mechanical diagnosis of rolling bearing faults in high-speed railroads.

**Keywords:** Incipient Failure Detection, Acoustic emission, Roller bearing, Diagnostic technique

Received on 17 February 2023, accepted on 28 August 2023, published on 19 September 2023

Copyright © 2023 Meng *et al.*, licensed to EAI. This open-access article is distributed under the terms of the [CC BY-NC-SA 4.0](https://creativecommons.org/licenses/by-nc-sa/4.0/), which permits copying, redistributing, remixing, transforming, and building upon the material in any medium so long as the original work is properly cited.

doi: 10.4108/ew.3908

\*Corresponding Author. Email: 101170084@ousn.edu.cn

### 1. Introduction

The development of science and technology has promoted the rapid growth of construction machinery, and mechanical equipment has gradually developed in the direction of automation and intelligence[1]. In high-speed trains, roller bearings determine the operational safety of high-speed trains, so it becomes essential to make automatic and accurate diagnoses of their internal faults[2]. Li Y uses machine learning to deeply analyze the real-time relevant fault diagnosis technology of the critical components of the electromechanical system of high-speed trains and puts forward a new automatic fault

diagnosis method based on genetic support vector machine[3]. Li Z et al. used the variational modal decomposition method. By decomposing the vibration signals of roller bearings using the variational modal decomposition method, they proposed a new automatic diagnosis method based on a random forest classifier and high spatial mode filter[4]. Liu Y Z et al. built the bearing abnormal temperature detection model and real-time prediction model based on the analytic hierarchy process by analyzing the relevant characteristics of the bearing temperature of high-speed trains under different times and spaces [5]. In this context, the research combines resonant failure detection (IFD) with the acoustic emission method (AE). It introduces the adaptive process of weighted fusion to fuse and analyze the data collected by the

sensors in two ways, aiming at improving the accuracy of automatic diagnosis of high-speed iron roller bearings and achieving pre-diagnosis.

The current research on automatic fault diagnosis methods for high-speed rail roller bearings is relatively simplistic. Therefore, combining AE and IFD methods and introducing weighted fusion adaptive ways are innovative. At the same time, the research is divided into four parts. The first part summarizes and discusses the current research on fault diagnosis of roller bearings. The second part analyzes automatic diagnosis technology for high-speed rail roller bearings, including the types and diagnostic methods of high-speed rail bearing faults and the analysis of IFD and AE methods. The third part is the performance verification of the fusion method, and the fourth part summarizes the entire article.

## 2. Related Work

Double-row tapered roller bearing is a critical component of high-speed railway, directly affecting high-speed trains' safe and stable operation. However, due to the high speed and high load of high-speed trains, the probability of failure is very high[6]. Therefore, improving the accuracy of automatic fault diagnosis becomes especially important, and in the bearing fault diagnosis, the IFD and AE methods are widely used[7]. Based on this, scholars at home and abroad have conducted in-depth research on this issue. Xiao X et al. constructed a framework for bearing fault diagnosis using a knowledge graph and data accumulation strategy to ensure the safe operation of high-speed rail roller bearings, effectively improving the diagnostic prediction accuracy and robustness of bearings based on the IFD method[8]. Wang H et al. extracted the early faint fault characteristics of rolling bearings accurately in the IFD method and frequency band method of multi-target information; they proposed an early fault feature enhancement method for rolling bearings, which effectively improved the accuracy of fault diagnosis and ensured the smooth operation of high-speed trains[9]. Gong T et al. proposed a new extraction method based on the adaptive stochastic IFD method to address the difficulty of extracting nonsmooth information of bearing faults under a robust noise environment so as that The feature information of the bearing is effectively enhanced based on the conversion of nonsmooth information into smooth details [10]. Guo J et al. used the IFD method to extract resonance information to realize feature extraction of the local fault of the rolling bearing. Based on the modulated signal bispectrum, a new fault diagnosis scheme is proposed, effectively improving the accuracy of bearing local fault diagnosis[11].

In addition, Hou D et al. proposed a new fault diagnosis method using the AE method and vibration analysis to ensure the overall safety of high-speed trains, thus realizing the early diagnosis of bearing faults in high-speed trains and improving their detection accuracy[12]. Aasi A et al. constructed a corresponding test device

based on AE sensors to realize the effective diagnosis of rolling bearing time-domain characteristics, thus effectively diagnosing rolling bearing defects and improving the stability of high-speed train operation[13]. Li Y et al. proposed a kernel entropy component analysis method with an enhanced moving window based on the AE method to improve the monitoring accuracy of mechanical structures based on obtaining more information on AE features[14]. Jawad S M et al. analyzed the vibration signals and constructed a bearing fault detection method based on the AE method to enhance the accuracy of machine health identification. To improve the health identification accuracy of the machine, Jawad S M et al. analyzed its vibration signal. They constructed a test bench for bearing fault identification based on the AE method, effectively reducing the frequency of machine running failures and improving fault detection accuracy [15].

From the research of domestic and foreign scholars, the current automatic diagnosis methods of roller bearing faults in high-speed railways are still relatively homogeneous. Therefore, the study combines the AE and IFD methods, which can more comprehensively and accurately diagnose the roller bearing faults. At the same time, the adaptive process of weighted fusion is introduced to effectively fuse the data collected by combining the two effectively, thus effectively enhancing the accuracy of diagnosis, which is highly innovative and practical in theory and practice.

## 3. Analysis of automatic diagnosis technology of high-speed railway roller bearings based on IFD and AE

### 3.1 Analysis of high-speed rail roller bearing fault types and diagnosis methods

To guarantee the safety and efficiency of high-speed railways in high-speed operation, the study constructs automatic diagnosis technology for roller bearings of high-speed railways based on the IFD and AE methods and verifies its effectiveness. A roller bearing is a kind of rolling bearing. As long as people understand its fault type and diagnosis method, they can fully appreciate its corresponding fault type and procedure, which are interrelated. Rolling bearing is a precision mechanical part that reduces friction loss by turning the sliding friction of the rotating shaft and the support into rolling friction. The main structure of a rolling bearing contains an outer ring, inner ring, rolling body, cage, etc.[16]. Generally speaking, the motion contact between the inner circle and the rolling body of the high-speed rail bearing is linear, so the two will be subject to considerable contact stress, and the load will also change periodically. When running into the load-bearing area, the bag will rapidly rise from 0 to the maximum and fall from zero to zero. Such load changes are likely to cause cracks in the outer ring and rolling element, which can lead to more

extensive failures and thus cause damage to the bearing. Among them, the failure types of rolling bearings of high-speed rail are shown in Figure 1.

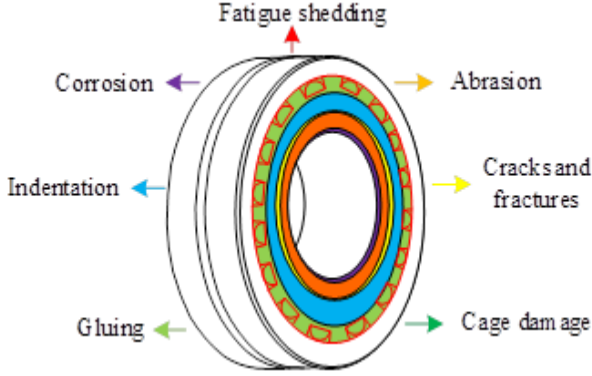


**Figure. 1 Fault Types of Rolling Bearing in High-speed Railway**

From Figure 1, high-speed rail's rolling bearing failure mainly contains fatigue shedding, wear, cracks and fractures, cage damage, gluing, indentation, and corrosion. In the actual working condition, the state of rolling bearings will be affected by many factors. The internal factors include the influence of the quality of the bearing material, the power of the bearing manufacturing process, and the impact of the bearing product design. External factors include installing and adjusting the overall machine of high-speed rail, maintenance, and maintenance repair in use. Under regular use, the outer ring of the bearing fits with the bearing housing and is connected in a fixed or relatively fixed way; the inner circle of the approach fits with the drive shaft of the mechanical device and drives the driving rod to rotate. Therefore, in the bearing operation, the vibration of the bearing will affect the overall performance of the path.

During the operation of a high-speed train, rolling the rolling body past these failure points produces a shock, which radiates rapidly outwards before the component is deformed. This longitudinal wave decays rapidly when the change occurs on the working surface of the element, resulting in a very brief, narrow pulse. However, a single rolling of adjacent rolling elements on the active surface of a component produces a relatively long interval of pulses, the corresponding frequency being called the "passing frequency." If the bearing has a fault, it is called the characteristic frequency of the spot [17]. The calculation equation is shown in Equation (1) and (2).

$$\begin{cases} f_0 = \frac{z}{2} f_r \left( 1 - \frac{d_1}{D_1} \cos \alpha \right) \\ f_1 = \frac{z}{2} f_r \left( 1 + \frac{d_1}{D_1} \cos \alpha \right) \\ f_g = \frac{D_1}{2d_1} f_r \left( 1 - \frac{d_1^2}{D_1^2} \right) \cos^2 \alpha \end{cases} \quad (1)$$

Equation (1)  $f_0$  indicates the relevant characteristic frequency when the outer ring fails;  $z$  shows the number of antifriction bearing rollers;  $f_r$  indicates the rotation frequency of the rolling bearing;  $d_1$  indicates the rolling body diameter of the antifriction bearing;  $D_1$  indicates the knuckle diameter of the antifriction bearing;  $\alpha$  indicates the pressure angle of the antifriction approach;  $f_1$  indicates the failure characteristic frequency of the inner ring.

$$\begin{cases} f_{bo} = \frac{f_r}{2} \left( 1 - \frac{d_1}{D_1} \cos \alpha \right) \\ f_{bi} = \frac{f_r}{2} \left( 1 + \frac{d_1}{D_1} \cos \alpha \right) \end{cases} \quad (2)$$

Equation (2)  $f_{bo}$  indicates the failure frequency when the rolling element contacts the outer ring and the cage contacts the inner circle. Therefore, diagnosing the failure of rolling bearings of high-speed rail becomes especially important when the failure occurs. The current bearing fault diagnosis method is shown in Figure 2.

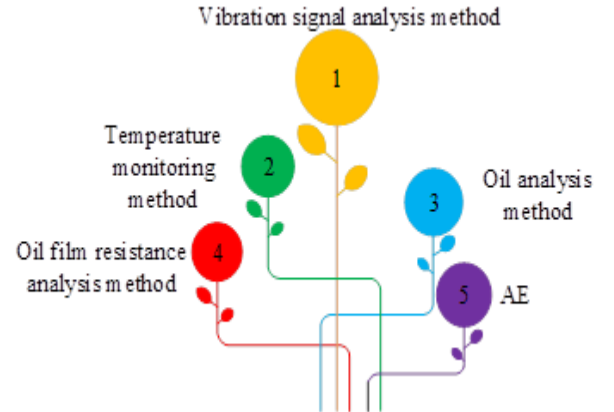


**Figure. 2 Classification of bearing fault diagnosis methods**

From Figure 2, the current fault diagnosis methods contain vibration signal analysis, temperature monitoring, oil analysis, oil film resistance, and AE detection methods. The vibration signal analysis method is more widely used for bearing fault diagnosis. When bearings are in operation, vibration will be caused by the influence of faults, and the greater the number of spots, the greater the vibration will be. From the side, it reflects that the pulse of the bearing contains a lot of fault information. Monitoring and analyzing faults by specific methods can get the fault information faster and more accurately. The IFD method chosen for the study is one of the vibration signal analysis methods. AE testing method is a kind of nondestructive testing technology. With the development of science and technology, many scholars also

increasingly value the research of AE testing methods [18].

### 3.2 High-speed rail double-row roller bearing IFD and AE technology research

In the actual rolling bearing detection and fault diagnosis, it is impossible to correctly determine its fault type by unthinkingly analyzing it without going through the fault mechanism and fault failure. Based on this, the study selects the IFD method to perform fault diagnosis on bearings. Its actual principle is shown in Figure 3.

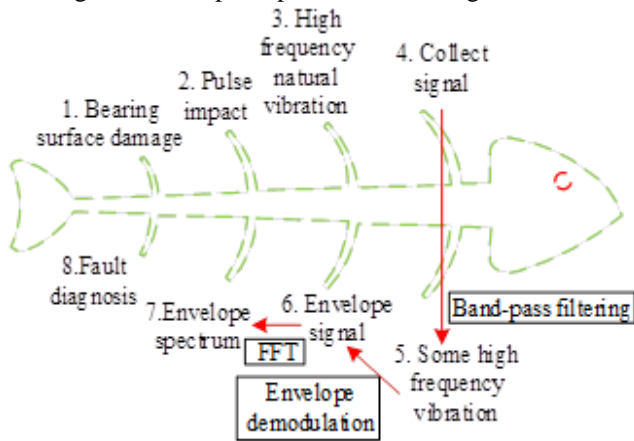


**Figure. 3 Practical principles of IFD technology**

In Figure 3, the FFT is the Fast Fourier Transform (FFT). From the Figure, the damaged part of the rolling bearing collides with the surface of other elements during operation, resulting in a pulse of concentrated energy and a specific frequency vibration. This lower periodic frequency resonates with the natural frequency of the bearing, and the complex high-frequency signal is extracted and then decomposed into low-frequency fault signals by Hilbert transform. Finally, FFT is used to process this signal accordingly to obtain the characteristics of the fault. Among them, the expression of Hilbert transform is shown in Equation (3).

$$\begin{cases} \hat{x}(t) = \frac{1}{t} \cdot x(t) = \frac{1}{\pi} \int_{-\infty}^{\infty} \frac{x(\tau)}{t-\tau} d\tau \\ \hat{x}(f) = X(f) \cdot F\left(\frac{1}{\pi}\right) = X(f) \cdot [-j \operatorname{sgn}(f)] \end{cases} \quad (3)$$

Equation (3)  $\hat{x}(t)$  denotes the transformed signal,  $t$  indicates the time,  $\tau$  means the time at the singularity,  $F$  denotes the equivalent static force,  $j$  denotes the signal order,  $f$  denotes the friction coefficient, and  $X$  denotes the sampled signal. Therefore, the amplitude and phase expressions of the resolved function of the movement  $x(t)$  are shown in Equation (4).

$$\begin{cases} |\tilde{x}(t)| = \sqrt{x^2(t) + \hat{x}^2(t)} \\ \theta(t) = \arctan\left(\frac{\hat{x}(t)}{x(t)}\right) \end{cases} \quad (4)$$

Equation (4)  $|\tilde{x}(t)|$  denotes the analytic function's amplitude and represents the rational function's phase. Based on this, Hilbert's instantaneous frequency definition expression is shown in Equation (5).

$$\omega = \frac{d\theta(t)}{dt} \quad (5)$$

Equation (5)  $\omega$  denotes the Hilbert instantaneous frequency. In the IFD method, the envelope detection technique is essentially the corresponding envelope demodulation of the signal. The IFD signal processing method is divided into low-pass filtering, Hilbert transform, and FFT. Low-pass filtering mainly extracts the low-frequency signal from the high-frequency signal, and then the Hilbert transform is used to remove the filtered signal further to obtain the low-frequency signal. At this time, the signals are time domain signals, which cannot make a correct judgment, and the Hilbert transform must be used to convert the time domain signals to frequency domain signals. The final frequency domain diagram is the spectrum diagram of the rolling bearing.

Thus, assume that  $x(t) = b(t)g(t)$   $b(t)$  denotes the

low-frequency signal and  $g(t)$  denotes the high-frequency signal. At this point, the Hilbert transform of the phase multiplication signal is mainly the bearing vibration signal obtained by the Hilbert transform of the high-frequency signal. The expression of the Hilbert transform of the bearing vibration signal is shown in Equation (6).

$$\hat{x}_j(t) = A_j \left[ 1 + \sum_{i=1}^n r_i \cos(2\pi f_r \cdot i \cdot t + \theta_i) \right] \sin(2\pi f_z \cdot j \cdot t + \phi_j) \quad (6)$$

Equation (6) represents the signal's peak value,  $n$  denotes the number of discrete sampling points in the time domain,  $r$  describes the rotational speed,  $i$  means the number of rolling elements,  $\theta_i$  indicates the angle of the rolling part  $\phi_i$ , and represents the transformed angle. Therefore, the signal obtained using the square root of Equation (6) is the envelope demodulated signal. This signal contains a low-frequency signal, which is the fault information of each component in the rolling bearing. The Hilbert transform can effectively eliminate the high-frequency signal in the low-frequency signal after low-frequency filtering and separate the low-frequency envelope information containing the fault information without affecting the characteristics of the original signal. In addition, when the relevant parts deform during the stress process, the elastic wave will generate strain

energy, which is the AE method. It uses the obtained acoustic signal to conduct nondestructive dynamic detection of the target or parts. The basic principle of AE monitoring of rolling bearings is shown in Figure 4.

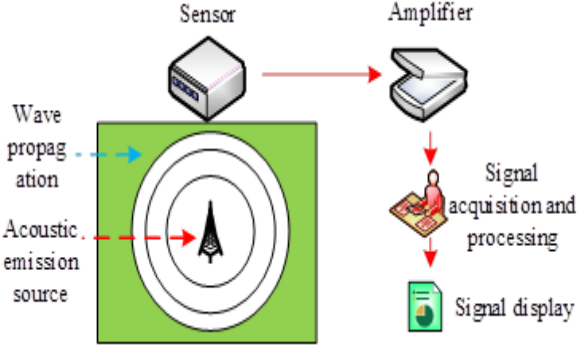


**Figure. 4 Basic principle of AE monitoring for rolling bearings**

In Figure 4, the elastic wave emitted by the sound source will have a certain displacement on the surface of the object, and when the movement speed of the thing exceeds the detection range of AE, it will convert it into an electronic signal. AE detection technology has characteristics that can detect the energy change through the device under test. No energy loss is generated in the detection process because the distance is too close. The fault information generated by AE itself is obtained from AE measurement, and no other equipment is needed for scanning. In addition, AE technology is a dynamic detection technology; it can't be used to detect static faults. AE signal is an elastic wave with a higher frequency, which has a broad spectrum and is less sensitive to the background noise in mechanical equipment. AE sensors are more prominent and require multiple vibration sensors to work together, thus reflecting its non-directional characteristics.

### 3.3 Analysis of adaptive weighted fusion algorithms in information fusion

The study uses the data obtained from multiple sensors under the IFD and AE methods in the actual fault diagnosis. To improve the measurement accuracy of rolling bearing faults, the study proposes a data-level fusion algorithm, namely, the adaptive weighted fusion method. The adaptive method of weighted fusion firstly performs the corresponding measurement and thus obtains the initialized value of the sensor; secondly, the initialized variance is calculated; then the optimal weight value is found using the initialization method; finally, the optimal weight value and the initialized value are multiplied to obtain the best deal after fusion. In the adaptive weighted fusion method, the relational expression of the weighting factor weights is shown in Equation (7).

$$\sum_{i'=1}^N k_{i'} = 1 \quad (7)$$

Equation (7)  $N$  denotes the number of sensors  $k_{i'}$  indicating the weighting factor's weight corresponding to the  $i'$  sensor. Therefore, the total variance expression of the data-weighted fusion result and the system's actual value waiting to be estimated is shown in Equation (8).

$$\begin{cases} \hat{B} = \sum_{i=1}^N k_i B_i \\ \sigma^2 = E \left[ (B - \hat{B})^2 \right] \end{cases} \quad (8)$$

Equation (8)  $\hat{B}$  represents the result of data weighting fusion,  $B_i$  represents the actual value of the corresponding system waiting for estimation,  $\sigma^2$  represents the total variance of this true value, and  $E$  represents the expected value. The expression obtained by substituting the value of  $\hat{B}$  Eq. (8) into the entire variance calculation formula is shown in Equation (9).

$$\begin{aligned} \sigma^2 &= E \left[ \left( \sum_{i=1}^N k_i B - \sum_{i=1}^N k_i B_i \right)^2 \right] = E \left[ \left( \sum_{i=1}^N k_i (B - B_i) \right)^2 \right] \\ &= E \left[ \sum_{i=1}^N k_i (B - B_i)^2 + 2 \sum_{i=1, j=1}^N k_i k_j (B - B_i)(B - B_j) \right] \end{aligned} \quad (9)$$

Equation (9)  $j'$  denotes the serial number of the sensor. Since each sensor's measurements are independent and unbiased estimates  $B$ , the average of positive and negative deviations is 0 in probability. The expression is shown in Equation (10).

$$E \left[ \sum_{i=1, j=1}^N k_i k_j (B - B_i)(B - B_j) \right] = 0 \quad (10)$$

Therefore, the expression obtained by substituting Equation (10) into Equation (9) is shown in Equation (11).

$$\sigma^2 = E \left[ \sum_{i=1}^N k_i^2 (B - B_i)^2 \right] = \sum_{i=1}^N k_i^2 \sigma_i^2 \quad (11)$$

In Equation (11), the total variance value is inversely related to the weighting factor, so the weighting factor's value is the best weight when the total variance value is the minimum value. The expression obtained by associating Eq. (7) and Eq. (11) and using the Lagrange multiplier method with partial derivative solution is shown in Equation (12).

$$\frac{\partial F'}{\partial k_i} = 2k_i \sigma_i^2 + \lambda \quad (12)$$

Equation (12)  $F'$  indicates that the external force the external field applies  $\lambda$  is the specific number of sensors. In this case, the left side of Equation (12) is set to 0, and

the expression obtained by summing is shown in Equation (13).

$$\lambda = -2 \frac{\sum_{i=1}^N k_i}{\sum_{i=1}^N \frac{1}{\sigma_i^2}} \quad (13)$$

On this basis, the expression of the extreme point obtained by substituting Equation (7) and Equation (13) into Equation (12) is shown in Equation (14).

$$k_i^* = \frac{1}{\sigma_i^2 \sum_{i=1}^N \frac{1}{\sigma_i^2}} \quad (14)$$

Equation (14)  $k_i^*$  denotes the extreme value point. The minimum value of the total variance can be obtained by substituting Equation (14) into Equation (11), and the final fusion result can be obtained by using the minimum value, whose expression is shown in Equation (15).

$$\hat{B}^* = \sum_{i=1}^N k_i^* B_i = \sum_{i=1}^N \frac{B_i}{\sigma_i^2 \sum_{i=1}^N \frac{1}{\sigma_i^2}} \quad (15)$$

Equation (15)  $\hat{B}^*$  denotes the final fusion result obtained. To compare the fused results more significantly, the study adds the optimal single-sensor fusion algorithm when performing the fusion analysis and considers multiple sensors with the minimum mean square error sensor as the fusion estimation.

#### 4. Example study of automatic fault diagnosis by information fusion of double-row roller bearings for high-speed rail

##### 4.1 Experimental data analysis of double row roller bearing IFD and AE technology

To verify the accuracy of the IFD and AE methods in automatic fault diagnosis of the double-row antifriction bearing of high-speed railways, the study first conducted corresponding fault diagnosis experiments on them. In the IFD method experiment, the study analyzed the outer ring faults of the bearings based on the collected data, and the spindle speeds of 350r/min and 1050r/min were selected. Among them, the diagnosis results of major and minor bearing faults at different rates are shown in Figure 5.

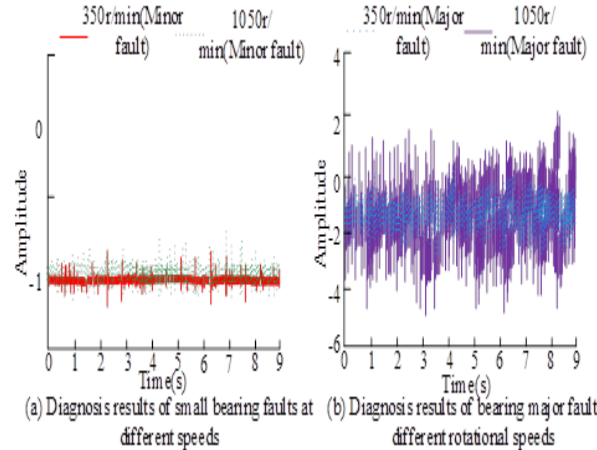


**Figure. 5 Diagnosis Results of Major and Minor Bearing Faults at Different Rotational Speeds**

From Figure 5(a), in the automatic diagnosis of minor faults, the increase in speed doesn't cause significant changes in the waveform, and the waveform amplitude remains roughly -1. Some of the waveform changes caused by the internal structure of the roller bearing and other mechanical systems are not very significant. From Figure 5(b), the waveform changes significantly in automatically diagnosing substantial faults. At 350 r/min speed, the waveform amplitude is maintained between -4 and 0. When the speed increases, the waveform amplitude reaches between -6 and 4. The waveform changes more significantly at the same speed due to the fault change. As the number of spots increases, the waveform amplitude increases, while the waveform amplitude becomes smaller at minor defects. The theory shows that the IFD method is more accurate in automatically diagnosing significant faults. To further verify this result, the resonance demodulation variation of the bearing at different speeds for major and minor defects was analyzed. The results are shown in Figure 6.

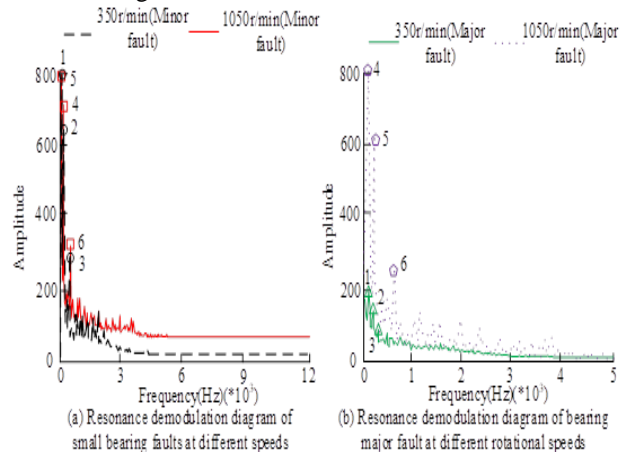


**Figure. 6 Resonance demodulation diagram of bearing fault at different speeds**

Comprehensive Figure 6 shows that the peak is more apparent when the fault size is the same, and the octave relationship is more evident when the bearing speed increases. However, the two-fold and three-fold frequencies do not meet the requirements at low speeds,

and at low rates, the three-fold frequency peaks are not prominent. At high speed, the octave relationship becomes more apparent. Especially at significant faults and high speeds, the 1-point frequency at 1050 rpm in Figure 6(b) is 172.4 Hz, which is very similar to the theoretical 176.9 Hz. The 2-point frequency at 1050 rpm is 347.6 Hz, and the 3-point frequency is 498.4 Hz, which are very close to the two- and three-fold frequencies of the 1-point frequency, and the multiplication relationship is much more straightforward. The comprehensive results show that the IFD method has high accuracy in automatically diagnosing significant faults at high speed. On this basis, the vibration waveforms of large and small spots at different rotational speeds collected using the AE method are studied, and the results are shown in Figure 7.

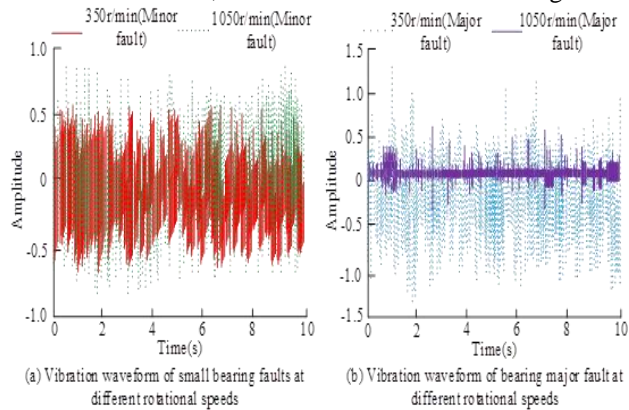


**Figure. 7 Vibration Waveforms of Bearing Faults at Different Rotational Speeds**

From Figure. 7(a), in the same type of failure, the waveform's amplitude varies more, the waveform becomes more significant with the increase of speed, and the waveform also undergoes more significant shocks. It's mainly because of the high energy stress wave caused by bearing dislodgement and collision of the rolling body. In the actual test, the waveform spacing is haphazard and irregular due to transmission loss and other reasons. From Figure 7(b), as the fault increases, the waveform's amplitude becomes more extensive, and more significant waveform shocks appear. It's mainly because of the increased rotational speed; the friction between the rolling element and the outer ring increases, which causes the stress energy to rise continuously, and the waveform shows periodic fluctuations. Overall, the AE method still generates many acoustic emission signals at low rotational speed and has higher effectiveness. To further verify the accuracy of the AE method in the automatic diagnosis of bearing faults, the study further analyzed the acquired signals to obtain the envelope spectrum, as shown in Figure 8.

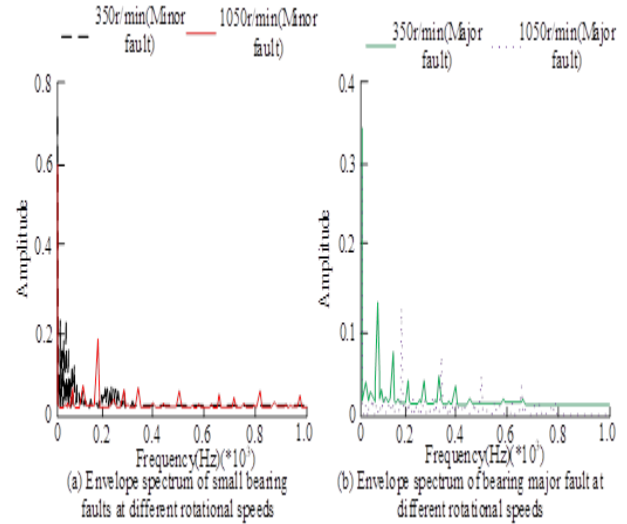


**Figure. 8 Envelope spectrum of bearing faults at different rotational speeds**

A comprehensive Figure 8 shows that the overall amplitude frequency is maintained between 0 and 1000 Hz. In addition, the maximum frequency of the amplitude is not significant when the bearing is running at low speed with a minor fault. The main reason is that when the experimental platform runs at low speed, its structural noise masks the fault signal, so the characteristic frequency of the fault cannot be extracted but can be roughly determined. As the rotational speed increases, the higher amplitude frequencies become more pronounced. At increasing responsibility, the maximum amplitude can be estimated even at lower speeds, while at more significant fault speed increases, the maximum amplitude is 174.8 Hz, comparable to the theoretical 176.9 Hz. Combining Figure 5 with Figure 8, it can be found that the overall measurement results of the AE method are more accurate, while the IFD method has a higher accuracy in extensive fault diagnosis. Therefore, the study combines its two methods to improve detection and automatic diagnosis accuracy and persuasiveness.

#### 4.2 Performance analysis of adaptive weighting algorithm under IFD and AE data fusion

The study proposes an adaptive weighting algorithm for data fusion of the two sensors when fusing AE and IFD methods. To verify its effectiveness, the study is divided into an algorithm that introduces the optimal single sensor fusion algorithm and arithmetic averaging, which is compared with the data fusion results of the adaptive weighting algorithm. The results are shown in Figure 9.

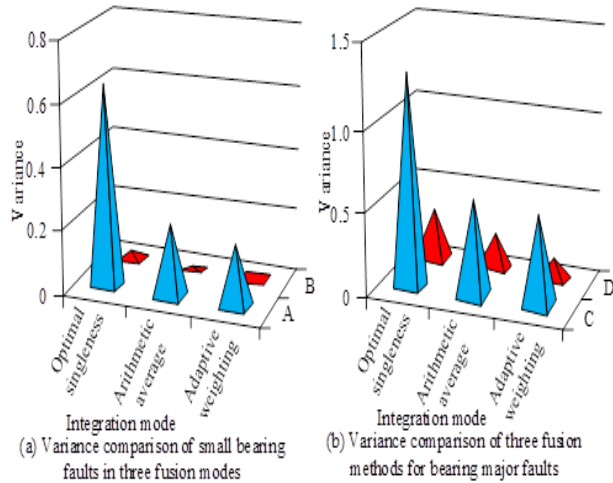


**Figure. 9 Comparison of bearing fault variance in three fusion modes**

In Figure 9, A-D denotes small-fault high-speed, small-fault-low-speed, large-fault high-speed, and large-fault-low-speed, respectively. From Figure 9(a), the variance of the optimal single-sensor fusion algorithm and the arithmetic average algorithm are 0.6546 and 0.2363, respectively, higher than the 0.2025 of the adaptive weighting algorithm in the small-fault high-speed diagnosis. Similarly, both are higher than the 0.0165 of the adaptive weighting algorithm in the small-fault low-speed diagnosis, indicating that their fusion effects are not ideal and their effectiveness is lower than that of the adaptive weighting algorithm. The variance of the optimal single-sensor fusion algorithm and the arithmetic average algorithm are 0.2892 and 0.1004, respectively, higher than the 0.0830 of the adaptive weighting algorithm in the large-fault low-speed diagnosis in Figure. 9(b).

Similarly, they are higher than the 0.5793 of the adaptive weighting algorithm in the large-fault high-speed diagnosis. It is more effective and shows that the multi-sensor combination of the IFD and AE methods is more accurate for the fault diagnosis of antifriction bearings. To further verify the results, the study compared the fusion results of the three fusion methods under the fault-free diagnosis of the path, and the results are shown in Figure 10.

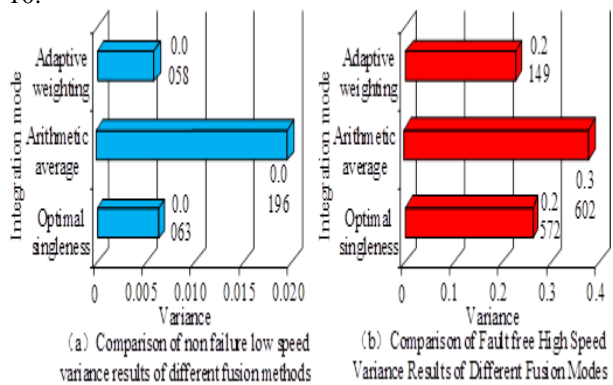


**Figure. 10 Comparison of fusion results of three fusion methods in bearing fault-free diagnosis**

Comprehensive Figure 10 shows that the variance of the adaptive weighting algorithm is 0.058 at low speed and 0.2149 at high speed for the fusion analysis of fault-free data, which are lower than the other two algorithms. It shows that the adaptive weighting algorithm effectively determines whether there is a fault in the bearing, i.e., the multi-sensor fusion combined with IFD and AE effectively diagnoses whether there is a fault in the direction. The combined Figure 9 and Figure 10 shows that the difference between the data with fewer faults and those without defects is minor. However, in practice, the difference between the two is still relatively significant whenever a flaw exists. Therefore, the combined method chosen for the study can be used to automatically pre-diagnose the bearing condition relatively quickly.

## 5. Conclusion

To automatically diagnose the fault status of high-speed roller bearings, the study combines IFD and AE and introduces an adaptive weighting algorithm to organically fuse both data while using relevant experiments to verify their effectiveness. The experimental results make clear that in the IFD method experiments, the waveform amplitude of the bearing minor fault diagnosis fluctuates around -1, and the primary fault diagnosis is maintained between -6 and 0. The frequency of 1 point under the large-fault high speed is 172.4 Hz, which is very similar to the theoretical 176.9 Hz. In the AE method experiment, the waveform's amplitude changes more in the same type of fault, and the waveform becomes more significant with increasing speed, and the waveform also undergoes larger shocks. The maximum amplitude of the waveform is 174.8 Hz at a more considerable fault speed increase, comparable to the theoretical 176.9 Hz. The IFD method has high accuracy for automatic diagnosis of significant faults, and the AE method has effectiveness for overall diagnosis, so the combination of the two is more comprehensive for analyzing the bearing condition. In the fusion method comparison experiment, the variance of the adaptive algorithm for high-speed diagnosis of minor faults in bearings is 0.2025 and 0.0165 for low speed, which is lower than the comparison algorithm. The results obtained in the fault-free diagnosis experiment are the same as those with faults. The combination of IFD and AE can diagnose the bearing condition more accurately and automatically; meanwhile, adding the adaptive weighted fusion algorithm can achieve pre-diagnosis. However, the study did not analyze the changes in its vibration waveform under data fusion, etc., which can be interpreted in depth in the follow-up.

## 6. Acknowledgement

This work is supported by the key technology research and application innovation research team of high-speed rail roller bearings No.TD2021004

## References

- [1] Wang X, Lv Z, Liu W, et al. Application Research on Mechanical Automation Technology in Mechanical Control [J]. *International Core Journal of Engineering*, 2022, 8(3): 47-50.
- [2] Liu Y, Wang B, Yang S, et al. Characteristic analysis of mechanical thermal coupling model for bearing rotor system of high-speed train [J]. *Applied Mathematics and Mechanics*, 2022, 43(9): 1381-1398.
- [3] Li Y. Exploring real-time fault detection of high-speed train traction motor based on machine learning and wavelet analysis [J]. *Neural Computing and Applications*, 2022, 34(12): 9301-9314.
- [4] Li Z, Lv Y, Yuan R, et al. An intelligent fault diagnosis method of rolling bearings via variational mode decomposition and standard spatial pattern-based feature extraction [J]. *IEEE Sensors Journal*, 2022, 22(15): 15169-15177.
- [5] Liu Y Z, Zou Y S, Wu Y, et al. A novel abnormal detection method for bearing temperature based on spatiotemporal fusion[J]. *Proceedings of the Institution of Mechanical Engineers, Part F: Journal of Rail and Rapid Transit*, 2022, 236(3): 317-333.
- [6] Zhao Y, Zhang J. Recent Patents on Detection of Bearing Temperature[J]. *Recent Patents on Engineering*, 2022, 16(3): 64-75.
- [7] Akhenia P, Bhavsar K, Panchal J, et al. Fault severity classification of ball bearing using SinGAN and deep convolutional neural network [J]. *Proceedings of the Institution of Mechanical Engineers, Part C: Journal of Mechanical Engineering Science*, 2022, 236(7): 3864-3877.
- [8] Xiao X, Li C, Huang J, et al. Fault Diagnosis of Rolling Bearing Based on Knowledge Graph With Data Accumulation Strategy[J]. *IEEE Sensors Journal*, 2022, 22(19): 18831-18840.
- [9] Wang H, Du W. Early weak fault diagnosis of rolling element bearing based on resonance sparse decomposition and multi-objective information frequency band selection method [J]. *Journal of Vibration and Control*, 2022, 28(19-20): 2762-2776.
- [10] Gong T, Yang J, Liu S, et al. Non-stationary feature extraction by the stochastic response of coupled oscillators and its application in bearing fault diagnosis under variable speed condition [J]. *Nonlinear Dynamics*, 2022, 108(4): 3839-3857.
- [11] Guo J, Shi Z, Zhen D, et al. Modulation signal bispectrum with optimized wavelet packet denoising for rolling bearing fault diagnosis [J]. *Structural Health Monitoring*, 2022, 21(3): 984-1011.
- [12] Hou D, Qi H, Luo H, et al. Comparative study on the use of acoustic emission and vibration analyses for the bearing fault diagnosis of high-speed trains [J]. *Structural Health Monitoring*, 2022, 21(4): 1518-1540.
- [13] Aasi A, Tabatabaei R, Aasi E, et al. Experimental investigation on time-domain features in the diagnosis of rolling element bearings by acoustic emission[J]. *Journal of Vibration and Control*, 2022, 28(19-20): 2585-2595.
- [14] Li Y, Xu F. Acoustic emission and moving window-improved kernel entropy component analysis for structural condition monitoring of hoisting machinery under various working conditions [J]. *Structural Health Monitoring*, 2022, 21(4): 1407-1431.
- [15] Jawad S M, Jaber A A. Bearings Health Monitoring Based on Frequency-Domain Vibration Signals Analysis [J]. *Engineering and Technology Journal*, 2022, 41(1): 86-95.
- [16] Fu W, Jiang X, Tan C, et al. Rolling Bearing Fault Diagnosis in Limited Data Scenarios Using Feature Enhanced Generative Adversarial Networks[J]. *IEEE Sensors Journal*, 2022, 22(9): 8749-8759.
- [17] Zhen D, Li D, Feng G, et al. Rolling bearing fault diagnosis based on VMD reconstruction and DCS demodulation [J]. *International Journal of Hydromechanics*, 2022, 5(3): 205-225.
- [18] Barile C, Casavola C, Pappalettera G, et al. Acoustic emission waveforms for damage monitoring in composite materials: shifting in spectral density, entropy and wavelet packet transform [J]. *Structural Health Monitoring*, 2022, 21(4): 1768-1789.